fractal and fractional

Article

The Fractal Characteristics of Soft Soil under Cyclic Loading Based on SEM

Bowen Kong [1,2,3,*], Chen-Xiang Dai [4], Haibo Hu [4], Jianzhong Xia [1] and Shao-Heng He [4,*]

1 School of Civil Engineering and Architecture, Zhejiang University of Science & Technology, Hangzhou 310023, China; 197002@zust.edu.cn
2 School of Physical and Mathematical Sciences, Nanjing Tech University, Nanjing 211816, China
3 Zhejiang Wuzhou Engineering Project Management Co., Ltd., Hangzhou 310053, China
4 Research Center of Coastal and Urban Geotechnical Engineering, Zhejiang University, Hangzhou 310058, China; 21912017@zju.edu.cn (C.-X.D.); huhaibo@zju.edu.cn (H.H.)
* Correspondence: kbw@zust.edu.cn (B.K.); heshaoheng@zju.edu.cn (S.-H.H.); Tel.: +86-137-3547-6567 (B.K.)

Abstract: Cyclic loading always results in great damage to the pore structure and fractal characteristics of soft soil. Scanning electron microscope (SEM) can help collect data to describe the microstructure of soft soil. This paper conducted a series of SEM tests to interpret the effect of consolidation confining pressure, circulating dynamic stress ratios and overconsolidation ratio on soil's micro-pore structure and fractal characteristics. The results demonstrate that fractal dimension can well represent the complex characteristics of the microstructure of the soil; the larger the consolidation confining pressure, the greater the cyclic dynamic stress ratio, and the greater the overconsolidation ratio, the smaller the fractal dimension number of soil samples. Finally, an empirical fitting formula for cumulative strain considering microstructure parameters is established through data fitting.

Keywords: soft soil; fractal characteristics; SEM; microstructure; cumulative strain

Citation: Kong, B.; Dai, C.-X.; Hu, H.; Xia, J.; He, S.-H. The Fractal Characteristics of Soft Soil under Cyclic Loading Based on SEM. *Fractal Fract.* **2022**, *6*, 423. https://doi.org/10.3390/fractalfract6080423

Academic Editor: Wojciech Sumelka

Received: 31 May 2022
Accepted: 26 July 2022
Published: 30 July 2022

1. Introduction

Marine-saturated silty soft clay is widely distributed in coastal areas, and is prone to settlement under long-term cyclic loads. Severe uneven settlement will cause damage to the superstructure and bring huge economic losses. Controlling the settlement of soft clay foundations is a key issue that needs to be solved urgently. Clarifying the deformation characteristics and microscopic mechanism of soft soil under dynamic load has great significance for the settlement control of soft soil foundation, so it is necessary to conduct systematic basic theoretical research.

Fractal theory is mainly used to study objects with self-similarity characteristics, which refer to the shape, function and feature information of the object. The plastic deformation parameters of fractional geomaterials have been studied extensively [1,2]. To explore the complexity of material composition, fractal theory was gradually widely used in the quantitative study of soil material composition [3–6]. In the past study of soil composition, fractal theory studies were mostly used to study the particle shape of sandy soil [7,8]. Delage R and Lefebvre G analyzed the distribution and arrangement of pores in the soil [9]. Peyton et al. and Zeng et al. used fractal theory to propose a microscopic difference conjecture that used fractal dimensions combined with fractal non-uniformity to describe soil structure [10,11]. He S et al. used fractal theory to study the distribution of soil pores, and the results showed that the pore structure in soil has fractal characteristics, which can be used to quantitatively describe the geometric characteristics of pore structure in the medium [12]. Wang P et al. explored the influence of electron microscopy factors on the quantitative study of microscopic information through a series of scanning electron microscopy pictures [13]. Kong B et al. carried out research on the fractal characteristics of soft soil under different temperatures and pressures [14].

However, existing research can mostly assist in explaining the reason of deformation causes and cannot quantify the relationship between macroscopic deformation and microscopic characteristic parameters. In order to find the precise quantitative relationship between micro and macro deformation, in this paper, the deformation of Hangzhou original soft clay was analyzed from a microscopic point of view under cyclic loading. With the help of SEM, the microstructure parameters of soil samples can be obtained [15]. Based on the existing empirical model of cumulative plastic strain index, the cumulative plastic strain model considering the microstructural parameters was established. Then, the correlation between microstructure parameters and cumulative plastic strain was calculated. The research results can be used as a reliable basis for predicting foundation deformation under cyclic loading by fractal dimension information.

2. Materials and Methods

2.1. Materials

The original soft soil samples were taken from the tunnel section of Zhejiang University's Zijingang Station and Sanba Station, which belongs to Hangzhou Metro Line 2. The maximum burial depth of the soil layer in this interval is 11.8 m, and the groundwater level is 1–2 m. The soil sample used in this test was about 5–5.5 m depth, which belongs to soft soil (based on USCS classification). The soil specimen was 40 mm in diameter and 40 mm in thickness (showed as Figure 1). The soil extraction processes were carried out in strict accordance with the relevant requirements, so the quality of soil samples could be effectively guaranteed.

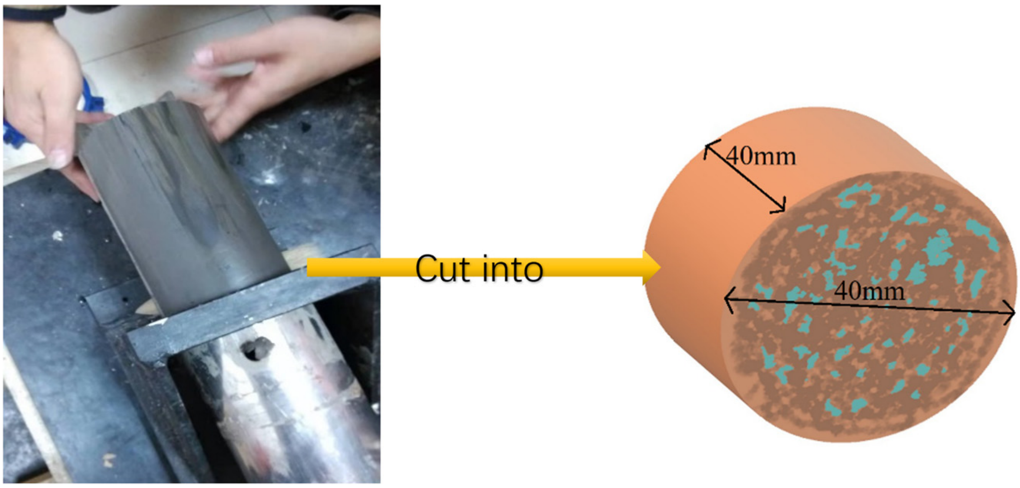

Figure 1. Photograph of undisturbed soft soil sample.

Basic physical and mechanical parameters of soil obtained through indoor geotechnical tests are shown in Table 1.

Table 1. Physical and mechanical parameters of soil.

Soil Type	Unit Weight/kN/m^3	Water Content/%	Specific Gravity	Plastic Limit/%	Liquid Limit/%	Plasticity Index	Liquid Index
Soft soil	15.7	62.47	2.74	27	44.6	17.6	2.01

2.2. Methods

The research includes two parts: firstly, the analysis of the macroscopic parameters (cumulative plastic strain) and microstructure parameters by SEM (fractal dimension and probability entropy). Secondly, based on the existing empirical model of cumulative plastic strain, the cumulative plastic strain model considering the microstructural parameters is established.

In this paper, the one-dimensional circulating load drainage consolidation test from Dai et al. [16] was adopted to provide new insight into the relationship between the microstructure and cumulative deformation. Consolidation conditions and cyclic loading conditions both have great influence on the soil fractal structure [17–19]. After determining the pre-consolidation pressure of the soil sample, the specimens were divided into three groups, namely Group A, Group B and Group C, which corresponded to different consolidation surrounding pressures P_0 (100, 200, 300, 400, 500 kPa); circulating dynamic stress ratios ζ (3, 6, 8, 10, 15); and overconsolidation ratios *OCR* (1, 3, 6, 9). Among them, specimens A_0, B_0, and C_0 represent the samples before loading (parallel specimens). In order to comprehensively explore the relationship between microporous structure and macroscopic mechanical properties, high stresses above 300 kPa were also considered. The experimental program is detailed in Table 2, where p_0 is pressure; ζ is cyclic dynamic stress ratio; N_{max} is the largest number of vibrations and *OCR* is overconsolidation ratio.

Table 2. Experimental program.

Group	Number	p_0/(kPa)	ζ	N_{max}	*OCR*
A	A0		not loaded		
	A1	100	3	20,000	1
	A2	200	3	20,000	1
	A3	300	3	20,000	1
	A4	400	3	20,000	1
	A5	500	3	20,000	1
B	B0		not loaded		
	B1	100	3	20,000	1
	B2	100	6	20,000	1
	B3	100	8	20,000	1
	B4	100	10	20,000	1
	B5	100	15	20,000	1
C	C0		not loaded		
	C1	100	3	20,000	1
	C2	300	3	20,000	3
	C3	600	3	20,000	6
	C4	900	3	20,000	9

Soil samples were saturated before the tests in vacuum equipment: air was sucked out to maintain negative pressure for 3 h, then airless water was added and samples were soaked for 12 h. The specimens were then consolidated under the consolidation surrounding pressure p_0. After the consolidation was completed, a one-dimensional cyclic load was applied to the specimen. Using a semi-sine wave as a stress waveform, the dynamic stress amplitude is p_f; the cyclic dynamic stress ratio ζ indicates the difference between the dynamic stress amplitude p_f, and the consolidation confining pressure p_0 ratio to the consolidation confining pressure p0, and $\zeta = (p_f - p_0)/p_0$. According to Table 1, the amplitude of cyclic dynamic stress pf can be obtained by determining the consolidation confining pressure p_0 and the cyclic dynamic stress ratio ζ. N refers to the number of loaded half-sine waves experienced, and the total number of vibrations is recorded as N_{max} (set N_{max} = 20,000). Vibration frequency in f refers to the reciprocal of each half-sine wave time course (set f = 0.1 Hz). The loading and waveform diagram is shown in Figure 2.

Scanning electron microscopy (SEM) was used to observe the marine soft soil under different dynamic load conditions (based on ASTM standard), as shown in Figure 3. Under the premise of ensuring that the observation surface was not disturbed, the sample was cut and polished into a 2 mm × 2 mm × 4 mm microscopic sample, and the loose float particles on the observation section were blown away with the ear ball. Along the height direction of the sample, a horizontal and vertical section were selected every 2 cm as the observation area. Due to the poor electrical conductivity of soft soil, in order to ensure the quality of microscopic images the surface of the dried sample was sprayed with 20–50 nm gold film as a conductive material. The SEM test used 8000 times magnification. The microstructure parameters were extracted using the software Image Pro-Plus 6.0 (referred to as IPP). The microstructure parameters were analyzed under different dynamic load conditions, and the contour boundaries of the soil sample shape were extracted to output pore characteristic data, including area, diameter, angle, orientation frequency, probabilistic entropy and fractal dimension.

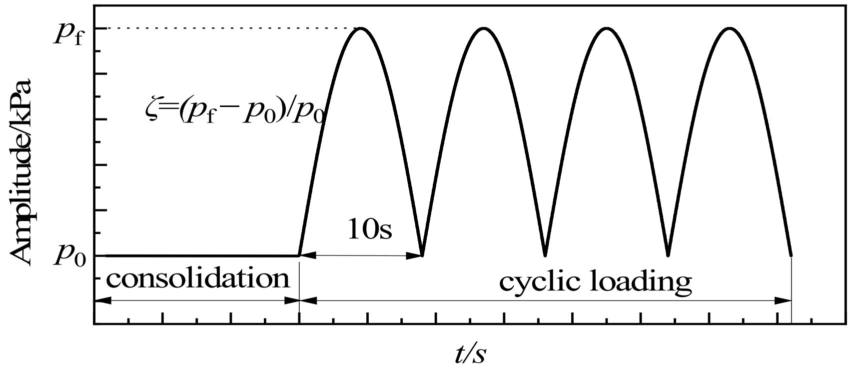

Figure 2. Loading and waveform diagram.

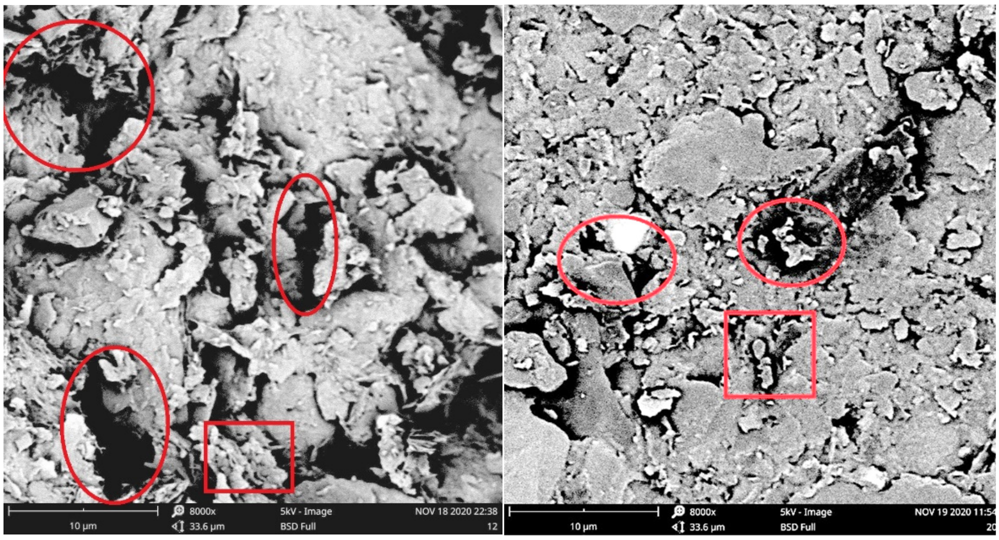

(**a**) (**b**)

Figure 3. Microscopic scanning images before and after loading [16]: (**a**) before loading; (**b**) after loading. *OCR* = 9 identifications of porosity units. (The circle was marked as a pore, and the square was marked as a flocculent structure).

The analysis has three steps [16]: first of all, a reference plane scale was created to convert the pixel units into length units; secondly, the images were binarized into black and white parts, where the black part represents soil grains and the white part represents pores (Figure 4a); finally, after the image was binarized, the system processing function of the IPP software was used to automatically collect image data (Figure 4b).

Based on the research results of Voss et al. [20], the fractal theory was introduced [21]. It was proposed that the area of particles in sandy soil images has the following relationship with the equivalent perimeter:

$$Log(Perimeter) = \frac{D_d}{2} \times Log(Area) + C \quad (1)$$

where Perimeter represents the equivalent perimeter of any geometric polygon in the scanned image; Area represents the equivalent area of the corresponding polygon; D_d

represents the fractal dimension of the particle shape of the soil corresponding to the scanned image; and C is a constant influenced by the microstructure characteristics of the material. The fractal information can be used both in microstructure and numerical simulation experiments [22].

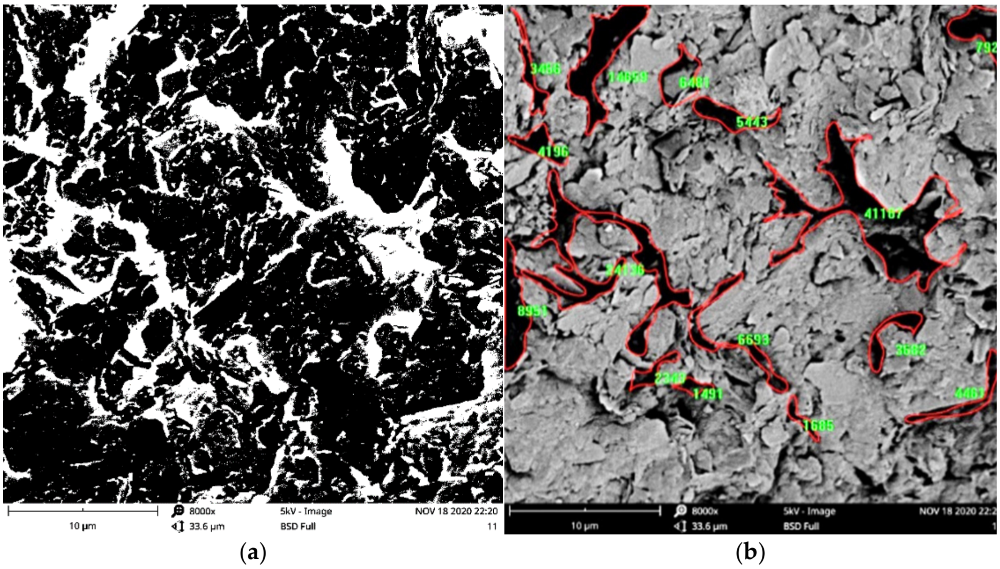

Figure 4. IPP picture processing [16]: (**a**) binary; (**b**) identification of porosity units (The pore contour and area are marked).

Shi Bin (1996) used modern systems theory to introduce the concept of probabilistic entropy into the study of soil's structure characteristics, and used H_m to describe the orderliness of the arrangement of soil microstructure units, defined as:

$$H_m = -\sum_{i=1}^{n} P_i(\alpha) \frac{\ln P_i(\alpha)}{\ln n} \tag{2}$$

where H_m represents probability entropy, which indicates the orderliness of the element body distribution, and P represents the probability of occurrence. The larger the H_m, the lower the order of the element arrangement.

3. Results

Figure 5a–c shows the cumulative strain curve of soil samples from Dai et al. [16]. It can be seen that in the early stage of cyclic load loading, an obvious squeezing effect occurs because the internal pores of the soil are subjected to load. When the vibration number increases to 10,000, the specimen is gradually compacted, and the strain accumulation rate is gradually slowed down, showing a slow growth trend. It can be inferred that in the process of vibration, the pore water is gradually discharged, resulting in the hardening of the soil structure. When the number of vibrations reaches a certain time (about 1000 times for the soil in this paper), the soil reaches a stable state and the cumulative strain tends to be stable.

With the continuous increase in the consolidation confining pressure and cyclic dynamic stress ratio, the final cumulative strain of the specimen gradually increases (Figure 5a,b). Under the same cyclic loads, high pressure or stress ratio were more conducive to the compaction of the soil, resulting in a faster strain accumulation rate, and a lager final cumulative strain. When the P_0 pressure reached 500 kPa, the cumulative strain value was twice of that at 100 kPa. The reason for this is that when the consolidation confining pressure and cyclic dynamic stress ratio are larger, the damage of the soil structure is aggravated.

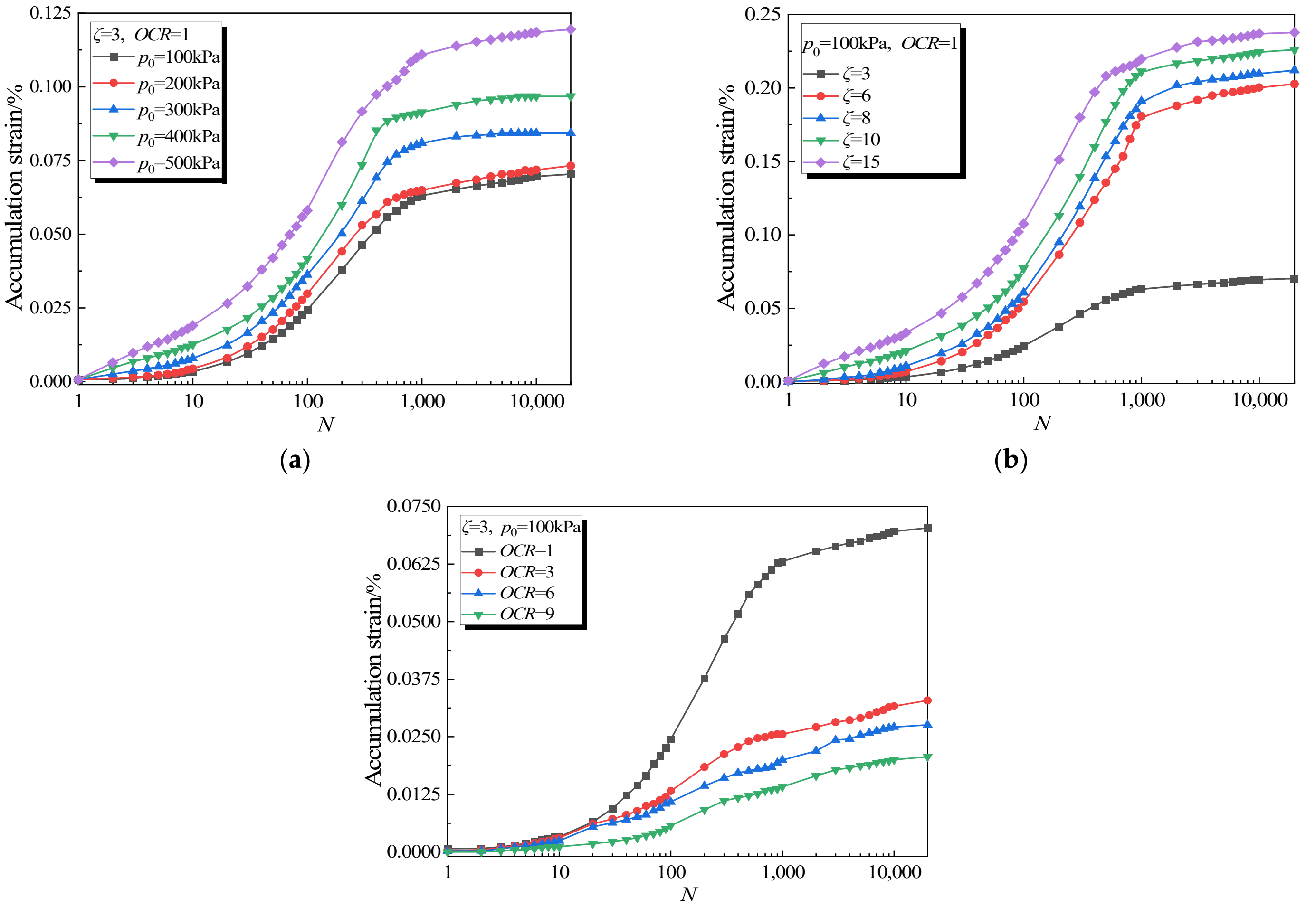

(**c**)

Figure 5. Cumulative strain-vibration curve in different dynamic load modes [16]: (**a**) group A; (**b**) group B; (**c**) group C.

It is worth noting that as the overconsolidation ratio continues to increase, the final cumulative strain of the specimen gradually decreases (Figure 5c). The reason is that under a high overconsolidation ratio the soil has a stronger resistance to deformation, resulting in a smaller final cumulative strain. This indicates that the increase in the overconsolidation ratio has an inhibitory effect on the cumulative strain.

Figures 6–8 show the *log* (*Perimeter*)-*log* (*Area*) curves of soft soil under different test conditions, which have obvious linear relationships. If the linear relationships are expressed as y = ax + b, then a in the linear relationships corresponds to D_d, and b corresponds to the perimeter in logarithmic coordinates. Therefore, it can be considered that the particle shape in soft clay is fractal. The number of fractal dimensions before loading is the largest (1.531 for the undisturbed soil sample), and the fractal dimension of soft soil is always between 1 and 2. After loading, the fractal dimension reaches 1. The results illustrate that the orderliness and directionality of the microstructure of soft soil are worst in the original state. After loading, with the reduction in the fractal dimension number, the pores become more orderly at any loading condition.

It can be seen that, with the increase in confine pressure, dynamic stress and ratio overconsolidation ratio, the fractal dimension value D_d decreased. The essence of the change of fractal dimension information is the change of the stress of the soil in equilibrium state under cyclic loading, which is caused by the recombination of particles in the soil and the dislocation movement of soil particles. In the early stage of loading, the soil particles moved in dislocation under cyclic loading, thus forming new pore structures. The accumulated energy of plastic strain dissipated, and the soil began to deform. With the increase in vibration N, the cumulative viscous energy dissipation rate gradually exceeds the cumulative plastic strain energy dissipation rate, the deformation tends to be stable, and the pore structure trends to be regular.

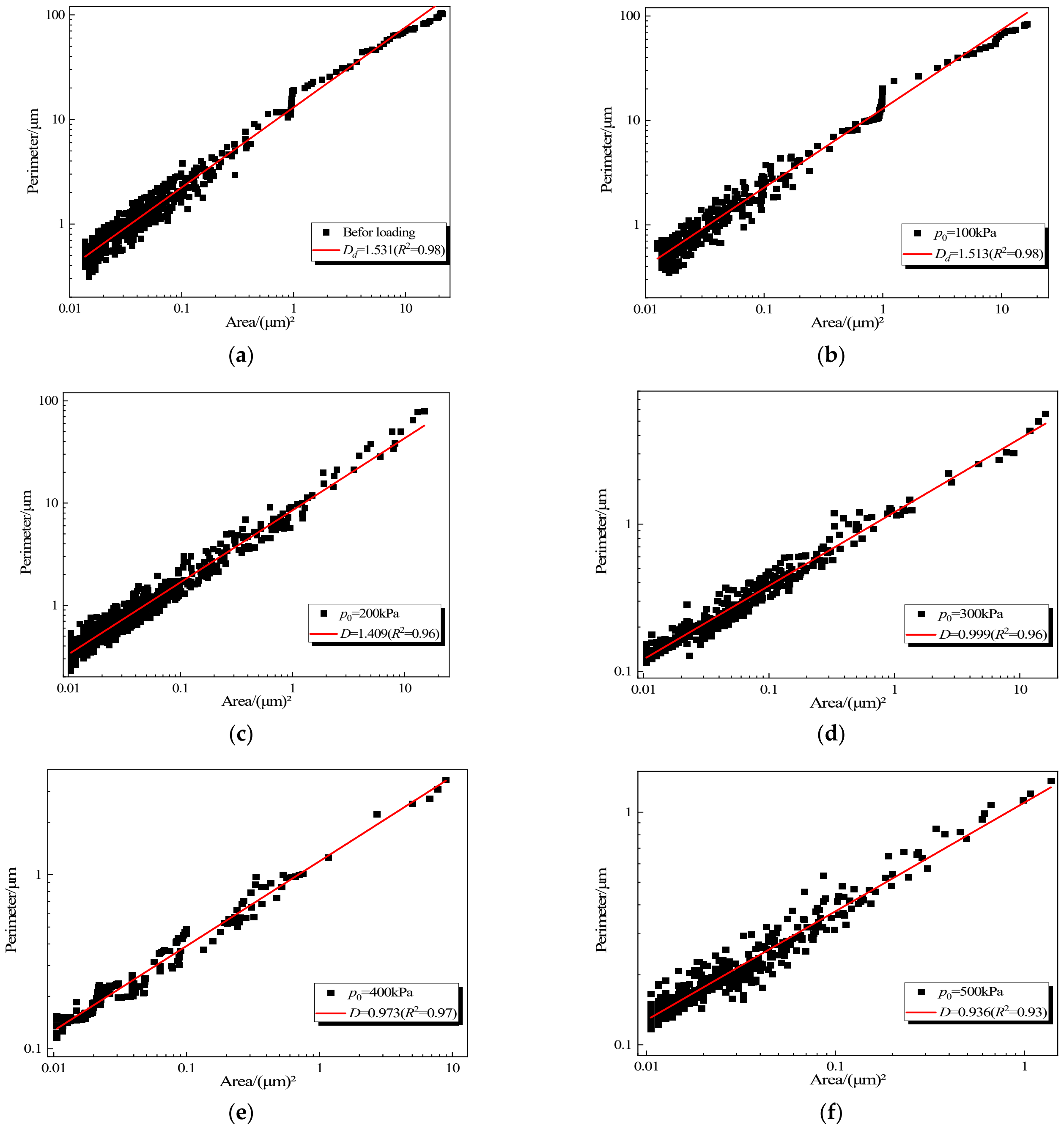

Figure 6. Fractal dimension of soil samples under different pressure: (**a**) before loading; (**b**) p_0 = 100 kPa; (**c**) p_0 = 200 kPa; (**d**) p_0 = 300 kPa; (**e**) p_0 = 400 kPa; (**f**) p_0 = 500 kPa.

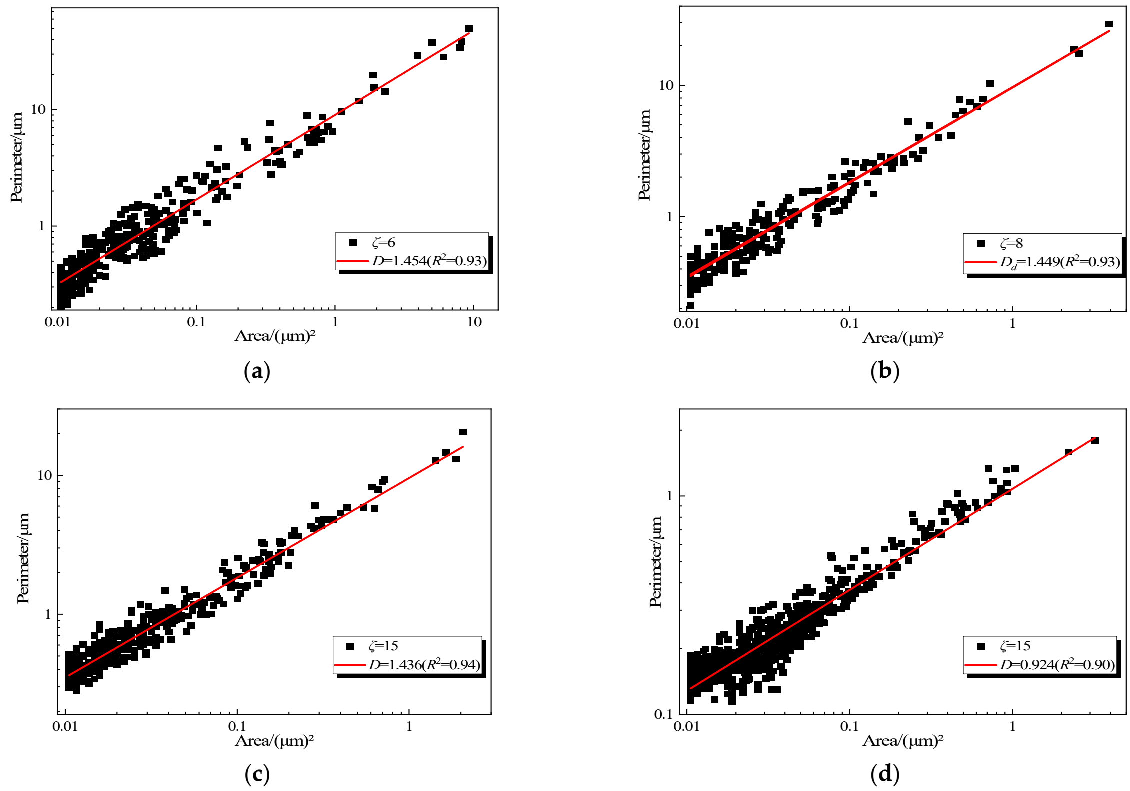

Figure 7. Fractal dimension of soil samples under different cyclic dynamic stress ratio: (**a**) ζ = 6; (**b**) ζ = 8; (**c**) ζ = 10; (**d**) ζ = 15.

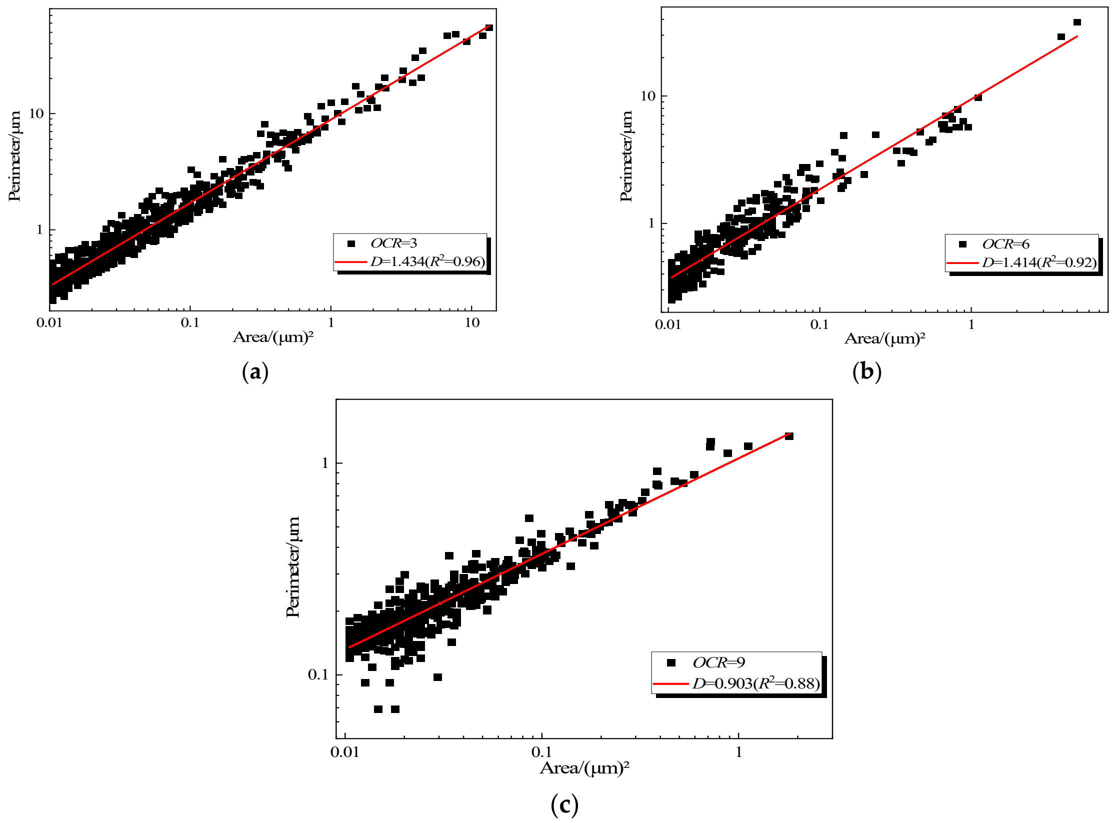

Figure 8. Fractal dimension of soil samples under different overconsolidation ratios: (**a**) *OCR* = 3; (**b**) *OCR* = 6; (**c**) *OCR* = 9.

4. Discussion

The macroscopic mechanical behavior of soil is closely related to the microinternal structure, so the microstructure changes of soft soil during cyclic loading can reveal the fundamental causes of its deformation.

At present, there are two main methods for calculating the cumulative plastic strain of soil under dynamic load: establishing a constitutive model and an empirical fitting formula. When calculating cumulative strain by constitutive model, it is difficult to determine the calculation parameters and apply in practical engineering. In contrast, the concise empirical fitting formulas are widely used in practical engineering.

Based on the Monismith exponential empirical model $\varepsilon = A \times N^b$ and the existing creep model [23], this paper introduces constant A_0 to reflect the stress σ and strain of soft soil ε:

$$\varepsilon(t) = A_0 + A \times t^b \tag{3}$$

where A_0, A, b represents the fitting constant.

Consider that A_0, A, b are parameters related to the stress state and the microstructural characteristics of the soil. Based on Formula (3), the cumulative plastic strain considering the microstructural parameters can be expressed as:

$$\varepsilon(t) = A_0(\sigma_i, C) + A(\sigma_i, C) \times t^{b(\sigma_i, C)} \tag{4}$$

where C is a series of microstructure characteristics of soft soil.

Since the shape of the cumulative strain curve at different stress levels also tends to be consistent; thus, $b(\sigma_i, C)$ can be considered as a constant β. The above formula can be simplified to:

$$\varepsilon(t) = E_0(\sigma_i, C) + E(\sigma_i, C) \times t^{\beta} \tag{5}$$

In Equation (5), $E_0(\sigma_i, C)$ is called the microstructure function, the value of which is related to the microstructure state of the soil at specific stress level. Therefore, if the probability entropy and fractal dimension are used as representatives of the microstructure parameters of soft soil, Equation (5) can be written as:

$$\varepsilon(t) = E_0(\sigma_i, H_\mathrm{m}) + E(\sigma_i, H_\mathrm{m}) \times t^{\beta m} \tag{6}$$

$$\varepsilon(t) = E_0(\sigma_i, D_d) + E(\sigma_i, D_d) \times t^{\beta d} \tag{7}$$

Let:

$$E(\sigma_i, H_m) = \left(\frac{\sigma_i}{A_m}\right)^{f_m(H_m)} \tag{8}$$

And

$$E(\sigma_i, D_d) = \left(\frac{\sigma_i}{A_d}\right)^{f_d(D_d)} \tag{9}$$

The exponential fitting empirical Equations (6) and (7) can be used to represent the orientation parameters of the soil structure. The calculation formula of cumulative plastic strain can be expressed as:

$$\varepsilon(t) = \left(\frac{\sigma_i}{A_{m0}}\right)^{f_m(H_m)} + \left(\frac{\sigma_i}{A_m}\right)^{f_m(H_m)} \times t^{\beta_m} \tag{10}$$

$$\varepsilon(t) = \left(\frac{\sigma_i}{A_{d0}}\right)^{f_d(D_d)} + \left(\frac{\sigma_i}{A_d}\right)^{f_d(D_d)} \times t^{\beta_d} \tag{11}$$

where A_m, A_{m0}, A_{d0} and A_d is the coefficient to be determined, $f_m(H_m)$, $f_d(D_d)$ is the probability entropy and fractal dimension function. Since the value of the function should be greater than 1 and $H_m \in [0,1]$, $D_d \in [0,1]$, the probability entropy and fractal dimension function can be expressed as:

$$f_m(H_m) = \frac{1}{H_m} \tag{12}$$

$$f_d(H_d) = \frac{1}{D_d} \tag{13}$$

where H_m, D_d is the probability entropy and fractal dimension. According to the change curve of probability entropy and fractal dimension with stress, the relationship between probability entropy and fractal dimension and stress can be expressed as follows:

$$H_m = a_m\sigma^2 + b_m\sigma + c_m \tag{14}$$

$$D_d = a_d\sigma^2 + b_d\sigma + c_d \tag{15}$$

where a_m, a_d, c_m, b_m, b_d and c_d are the fitted values of the probability entropy H_m and fractal dimension D_d and stress σ.

Then, Equations (12) and (13) can be expressed as:

$$f_m(H_m) = \frac{1}{a_m\sigma^2 + b_m\sigma + c_m} \tag{16}$$

$$f_d(D_d) = \frac{1}{a_d\sigma^2 + b_d\sigma + c_d} \tag{17}$$

Based on Equations (16) and (17), Equations (10) and (11) can be written as:

$$\varepsilon(t) = \left(\frac{\sigma_i}{A_{m0}}\right)^{\frac{1}{a_m\sigma^2 + b_m\sigma + c_m}} + \left(\frac{\sigma_i}{A_m}\right)^{\frac{1}{a_m\sigma^2 + b_m\sigma + c_m}} \times t^{\beta_m} \tag{18}$$

$$\varepsilon(t) = \left(\frac{\sigma_i}{A_{d0}}\right)^{\frac{1}{a_d\sigma^2 + b_d\sigma + c_d}} + \left(\frac{\sigma_i}{A_d}\right)^{\frac{1}{a_d\sigma^2 + b_d\sigma + c_d}} \times t^{\beta_d} \tag{19}$$

According to the experimental data of the probabilistic entropy and fractal dimension above, the value of parameters can be obtained in Table 3.

Table 3. Summary of parameters.

Parameter	a_m	b_m	c_m		a_d	b_d		c_d
numeric value	-1.279×10^{-7}	-4267×10^{-5}	0.9834		3831×10^{-7}	-0.0016		1.597
Parameter	A_{m0}	A_m	β_m	R^2	A_{d0}	A_d	β_d	R^2
numeric value	9.451×10^5	1.871×10^7	10.98	0.8396	7.106×10^4	981.5	-1.76	0.9629

As shown in Figure 9, the formula of cumulative plastic strain with fractal dimension as the microstructural parameter has a higher correlation coefficient (0.9629) than the formula with probabilistic entropy (0.8396) as the microstructure parameter. Consequently, the fractal dimension can describe the cumulative plastic strain law of Hangzhou's soft soil more accurately. In future studies, other microstructural parameters could be investigated to make the fitted formula curve closer to the experimental data.

Therefore, this paper introduces the fractal dimension as a microstructure parameter into the cumulative strain formula:

$$\varepsilon(t) = \left(\frac{\sigma_i}{A_{d0}}\right)^{\frac{1}{a_d\sigma^2 + b_d\sigma + c_d}} + \left(\frac{\sigma_i}{A_d}\right)^{\frac{1}{a_d\sigma^2 + b_d\sigma + c_d}} \times t^{\beta_d} \tag{20}$$

where a_d, b_d, c_d, A_{d0}, A_d and β_d are test fitting parameters.

Overall, fractal dimension information from soft soil provides a reliable method to obtain strain, which is helpful when predicting the physical and mechanical properties. The impact of various confine pressures, cyclic dynamic stress ratio and *OCR* were obtained from the analysis of the test results, which describe the fractal characteristics of soft soil. The mathematical relationship between the fractal characteristics and deformation characteristics deserves further investigation.

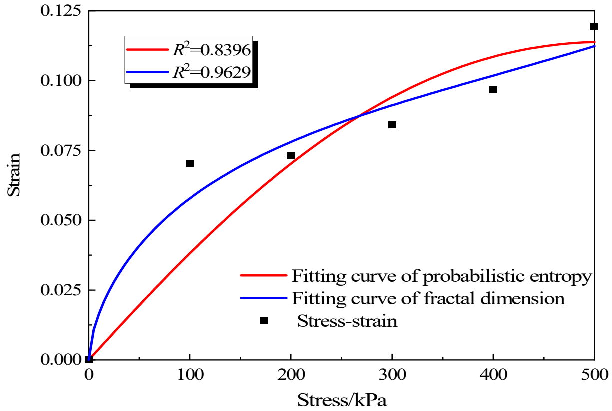

Figure 9. Fitting results by probability entropy and fractal dimension.

5. Conclusions

Using SEM technology, the microstructural change in soft soil under loading was observed, and the fractal dimension of pores was calculated by image processing techniques. Then, the relationship between microporous structure and macrodynamic characteristics were studied by using correlation and empirical model analysis methods. The relationship between the microstructure parameters obtained by SEM and the cumulative strain was discussed. Finally, the following main conclusions were drawn:

(1) The soft soil of Hangzhou marine has a flocculation structure. The distribution of soil particles in the microstructure of soft clay conforms to the fractal characteristics, and the fractal dimension number is between 1 and 2.

(2) After loading, the pores become more orderly. The larger the consolidation confining pressure, the greater the cyclic dynamic stress ratio and the greater the overconsolidation ratio, the smaller the fractal dimension number of soil samples.

(3) Fractal dimension and probabilistic entropy are closely related to cumulative strain. Based on the empirical fitting formula of strain index, an empirical fitting formula for cumulative strain considering microstructure parameters was established.

(4) The trends from the fractal dimension and probabilistic entropy are consistent with each other. The accuracy of the predicted probabilistic entropy strain is 0.83, whereas this value is 0.96 for the fractal dimension. Then, a new way to predict subsidence based on fractal dimension information was obtained for soft soil.

Author Contributions: Conceptualization, B.K. and C.-X.D.; methodology, B.K.; validation, C.-X.D.; formal analysis, B.K. and H.H.; investigation, C.-X.D.; resources, S.-H.H.; data curation, S.-H.H.; writing—original draft preparation, B.K.; writing—review and editing, B.K. and H.H.; visualization, S.-H.H.; supervision, J.X.; project administration, J.X.; funding acquisition B.K. and J.X. All authors have read and agreed to the published version of the manuscript.

Funding: National Natural Science Foundation of China (No. 52008373); Zhejiang Science and Technology Plan Project (2022C35026).

Institutional Review Board Statement: Not applicable.

Informed Consent Statement: Not applicable.

Data Availability Statement: The data are available from the corresponding author upon request.

Acknowledgments: The authors are very grateful to Yifei Sun from Ruhr University Bchum for his kind guidance in writing this article.

Conflicts of Interest: The authors declare no conflict of interest.

References

1. Sun, Y.F.; Sumelka, W. Bounding surface model refined with fractional dilatancy relation for sand. *Soils Found.* **2022**, *62*, 101149. [CrossRef]
2. Sumelka, W.; Blaszczyk, T. Fractional continua for linear elasticity. *Arch. Mech.* **2014**, *66*, 147–172.
3. Li, Y.; Zhang, H.; Huang, M.; Yin, H.; Jiang, K.; Xiao, K.; Tang, S. Influence of Different Alkali Sulfates on the Shrinkage, Hydration, Pore Structure, Fractal Dimension and Microstructure of Low-Heat Portland Cement, Medium-Heat Portland Cement and Ordinary Portland Cement. *Fractal Fract.* **2021**, *5*, 79. [CrossRef]
4. Pfeifer, P.; Avnir, D. Chemistry in noninteger dimensions between two and three. I. Fractal theory of heterogeneous surfaces. *J. Chem. Phys.* **1983**, *79*, 7. [CrossRef]
5. Zhao, X.; Yang, B.; Yuan, S.; Shen, Z.; Feng, D. Seepage–Fractal Model of Embankment Soil and Its Application. *Fractal Fract.* **2022**, *6*, 277. [CrossRef]
6. Fu, X.; Ding, H.; Sheng, Q.; Zhang, Z.; Yin, D.; Chen, F. Fractal Analysis of Particle Distribution and Scale Effect in a Soil–Rock Mixture. *Fractal Fract.* **2022**, *6*, 120. [CrossRef]
7. Zhou, S.; Liu, D.; Cai, Y.; Yao, Y. Fractal characterization of pore–fracture in low-rank coals using a low-field NMR relaxation method. *Fuel* **2016**, *181*, 218–226. [CrossRef]
8. Sun, W.; Zuo, Y.; Wu, Z.; Liu, H.; Xi, S.; Shui, Y.; Wang, J.; Liu, R.; Lin, J. Fractal analysis of pores and the pore structure of the Lower Cambrian Niutitang shale in northern Guizhou province: Investigations using NMR, SEM and image analyses. *Mar. Pet. Geol.* **2018**, *99*, 416–428. [CrossRef]
9. Delage, P.; Lefebvre, G. Study of the structure of a sensitive Champlain clay and of its evolution during consolidation. *Can. Geotech. J.* **1984**, *21*, 21–35. [CrossRef]
10. Peyton, R.L.; Gantzer, C.J.; Anderson, S.H.; Haeffner, B.A.; Pfeifer, P. Fractal dimension to describe soil macropore structure using X ray computed tomography. *Water Resour. Res.* **1994**, *30*, 691–700. [CrossRef]
11. Zeng, Y.; Payton, R.L.; Gantzer, C.J.; Anderson, S.H. Fractal Dimension and Lacunarity of Bulk Density Determined with X-ray Computed Tomography. *Soil Sci. Soc. Am. J.* **1996**, *60*, 1718–1724. [CrossRef]
12. He, S.-H.; Ding, Z.; Hu, H.-B.; Gao, M. Effect of Grain Size on Microscopic Pore Structure and Fractal Characteristics of Carbonate-Based Sand and Silicate-Based Sand. *Fractal Fract.* **2021**, *5*, 152. [CrossRef]
13. Wang, P.; Jiang, Z.; Ji, W.; Zhang, C.; Yuan, Y.; Chen, L. Heterogeneity of intergranular, intraparticle and organic pores in longmaxi shale in Sichuan basin, south China: Evidence from SEM digital images and fractal and multifractal geometries. *Mar. Pet. Geol.* **2016**, *72*, 122–138. [CrossRef]
14. Kong, B.; He, S.-H.; Tao, Y.; Xia, J. Pore Structure and Fractal Characteristics of Frozen–Thawed Soft Soil. *Fractal Fract.* **2022**, *6*, 183. [CrossRef]
15. Yang, R.; He, S.; Yi, J.; Hu, Q. Nano-scale pore structure and fractal dimension of organic-rich Wufeng-Longmaxi shale from Jiaoshiba area, Sichuan Basin: Investigations using FE-SEM, gas adsorption and helium pycnometry. *Mar. Pet. Geol.* **2015**, *7*, 27–45. [CrossRef]
16. Dai, C.-X.; Zhang, Q.-F.; He, S.-H.; Zhang, A.; Shan, H.-F.; Xia, T.-D. Variation in micro-pores during dynamic consolidation and compression of soft marine soil. *J. Mar. Sci. Eng.* **2021**, *9*, 750. [CrossRef]
17. Cai, Y.Q.; Hao, B.B.; Gu, C.; Wang, J.; Pan, L.Y. Effect of anisotropic consolidation stress paths on the undrained shear behavior of reconstituted Wenzhou clay. *Eng. Geol.* **2018**, *242*, 23–33. [CrossRef]
18. Yuan, B.; Li, Z.; Chen, W.; Zhao, J.; Lv, J.; Song, J.; Cao, X. Influence of Groundwater Depth on Pile–Soil Mechanical Properties and Fractal Characteristics under Cyclic Loading. *Fractal Fract.* **2022**, *6*, 198. [CrossRef]
19. Bohaienko, V.; Bulavatsky, V. Fractional-Fractal Modeling of Filtration-Consolidation Processes in Saline Saturated Soils. *Fractal Fract.* **2020**, *4*, 59. [CrossRef]
20. Voss, R.F.; Laibowitz, R.B.; Alessandrini, E.I. *Fractal Geometry of Percolation in Thin Gold Films*; Springer: New York, NY, USA, 1991.
21. Moore, C.A.; Donaldson, C.F. Quantifying soil microstructure using fractals. *Geotechnique* **1995**, *45*, 105–116. [CrossRef]
22. Sumelka, W.; Nowak, M. Non-normality and induced plastic anisotropy under fractional plastic flow rule: A numerical study. *Int. J. Numer. Anal. Methods Geomech.* **2016**, *40*, 651–675. [CrossRef]
23. Zhang, M.J.; Zhang, L.P. The study on the licrostructure parameters and rheological constitutive relations of structural soft soils. *J. Shenyang Jianzhu Univ. Nat. Sci. Ed.* **2006**, *22*, 177–180.